Research Square

Preprints are preliminary reports that have not undergone peer review.
They should not be considered conclusive, used to inform clinical practice,
or referenced by the media as validated information.

Ginger essential oil and citral ameliorate atherosclerosis via modulating TMAO and gut microbiota in ApoE−/− mice fed on Gubra amylin NASH diet with β-carnitine

Lee-Yan Sheen (lysheen@ntu.edu.tw)
National Taiwan University https://orcid.org/0000-0001-5541-652X

Suraphan Panyod
National Taiwan University https://orcid.org/0000-0001-8998-375X

Wei-Kai Wu
National Taiwan University Hospital

Sin-Yi Peng
National Taiwan University

Yea-Jing Tseng
National Taiwan University

Ya-Chi Hsieh
National Taiwan University

Rou-An Chen
National Taiwan University

Huai-Syuan Huang
National Taiwan University

Yi-Hsun Chen
National Taiwan University

Hsiao-Li Chuang
National Applied Research Laboratories

Cheng-Chih Hsu
National Taiwan University

Ting-Chin David Shen
Perelman School of Medicine, University of Pennsylvania

Kai-Chien Yang
National Taiwan University

Chi-Tang Ho
Rutgers University

Ming-Shiang Wu
National Taiwan University Hospital

Article

Keywords: atherosclerosis, -carnitine, gut microbiota, TMAO, GAN diet, ginger essential oil

Posted Date: November 17th, 2022

DOI: https://doi.org/10.21203/rs.3.rs-2247634/v1

License: This work is licensed under a Creative Commons Attribution 4.0 International License.
Read Full License

Abstract

Gut microbiota and its metabolites, along with host metabolism of -carnitine, play a crucial role in cardiovascular disease (CVD) development, forming Trimethylamine-N-oxide (TMAO), an atherosclerosis risk factor. TMAO promotes the formation of atherosclerotic plaques and platelet aggregation potential, causing thrombosis. A high-fat diet and carnitine administration can accelerate CVD progression. Ginger (*Zingiber officinale* Roscoe) essential oil (GEO) and its bioactive compound citral have lipid lowering and anti-inflammatory effects, which may prevent CVD; however, their ability to prevent atherosclerosis through gut microbiota modulation remains to be elucidated. Furthermore, the Gubra Amylin NASH (GAN) diet is a palm oil-containing high-fat diet for inducing steatohepatitis; however, the study of the GAN diet in combination with -carnitine for inducing atherosclerosis in mouse model has not been investigated yet. We examined the CVD-protecting effect of GEO and citral against the formation of aortic atherosclerosis and linked them with changes in the gut microbiota and its metabolites in the -carnitine/GAN diet-treated apolipoprotein E-deficient ($ApoE^{-/-}$) mouse model. GEO and citral demonstrated CVD protective function by alleviating aortic atherosclerotic lesions. They reduced blood sugar, improved insulin resistance, decreased plasma TMAO levels, and inhibited serum inflammatory cytokines, especially interleukin-1β. Moreover, they demonstrated their ability to modulate gut microbiota diversity and composition into a favourable direction. Collectively, GEO and citral may serve as potential prebiotics for CVD prevention by improving dysbiosis.

Introduction

Cardiovascular disease (CVD) is the most severe health problem worldwide and one of the leading causes of death globally.[1] The primary causes of CVD are, an unhealthy diet and insufficient physical activity.[2] The gut microbiota and its metabolites are strongly associated with dietary intake and have recently been proved as an emerging risk factor for CVD.[3] High animal-protein consumption has always been associated with CVD,[4] being the primary source of CVD risk factor precursors.[3] Several food components from red meat, poultry, and dairy products, such as phosphatidylcholine, choline, and -carnitine, can be metabolized through metaorganismal metabolism involving a specific gut microbiome and host to form γ-butyrobetaine (γBB), trimethylamine (TMA), and trimethylamine-N-oxide (TMAO).[5] Moreover, TMA can be subsequently oxidized to TMAO by the host hepatic flavin monooxygenase.[6] High blood TMAO levels are associated with cardiovascular events and all-cause mortality.[7] The atherogenic effects of TMAO include increased foam cell formation, reduced reverse cholesterol transport, enhanced platelet aggregation, and promotion of kidney fibrosis.[6, 8, 9] TMAO also causes vascular inflammation.[10]

Obesity is strongly linked to CVD.[11] In animals, mice fed a high-fat diet (HFD) show markedly elevated circulating TMAO levels associated with cardiac dysfunction. [12] An HFD animal model is essential for studying the gut-liver axis by creating a gut microbiota imbalance and subsequently increasing harmful metabolite production.[13] A novel Western diet pattern called the Gubra Amylin NASH diet (GAN diet) is characterized by 40 kcal% fat (primarily from palm oil), 20 kcal% fructose, and 2% cholesterol.[14] The GAN

diet mouse model exhibits the advantage of translatability to humans in terms of liver biopsy phenotype.[15] Thus, combining the GAN diet with -carnitine may potentially elevate blood TMAO levels and allow further investigation of the atherosclerosis-related mechanisms. An atherosclerosis-prone apolipoprotein E-deficient ($ApoE^{-/-}$) mouse model is a valuable tool for studying the development of atherosclerotic plaques. $ApoE^{-/-}$ mice are deficient in the ability to clear lipoproteins, resulting in the accumulation of cholesterol ester-enriched particle in blood, which can enhance atherosclerosis.[16]

Preventive medicine is the practice of promoting preventive health care to avert disease development. Several foods and herbs can alleviate the progression of CVD and atherosclerosis.[3,17] Ginger is a herbal dietary component with potential benefits against CVD. It has several advantageous effects on health, including reduction in total blood cholesterol and pro-inflammatory cytokine levels along with improved insulin resistance.[18] Ginger essential oil (GEO), the volatile oil obtained from fresh ginger, can reduce serums levels of cholesterol and triglycerides as well as insulin in HFD-induced obese mice.[19] In addition, citral is one of the primary components of GEO exhibiting anti-obesity activity.[19] GEO also ameliorates liver inflammation through mediated NLR family pyrin domain-containing 3 inflammasome (NLRP3) and modulating gut microbiota-lipopolysaccharide (LPS)/toll-like receptor 4 (TLR4) signalling pathways in the GAN diet-induced non-alcoholic steatohepatitis (NASH) mouse model. In addition, GEO boosts the beneficial microbiome but reduces NASH-associated microbiota.[20] However, there are limited studies on the effect of GEO and citral in preventing atherosclerosis by modulating the gut microbiota and its metabolite TMAO; therefore, we aimed to assess these effects on GAN diet/ -carnitine-induced atherosclerosis in $ApoE^{-/-}$ mice.

Results

GEO and citral protect against atherosclerosis and improve plasma lipidaemic biomarkers

To examine the protective effect of GEO and citral against CVD and atherosclerosis, the $ApoE^{-/-}$ mice were fed a GAN/ -carnitine (GC) diet—1·3% in water, supplemented with two doses of GEO—Low: 50 mg/kg bw and High: 100 mg/kg bw, or citral—20 mg/kg bw (Fig. 1a). These supplements were administrated daily to the $ApoE^{-/-}$ mice. After 16 weeks, the mice were sacrificed and aortic lesions were visualized after dissection and staining with oil red O dye (Fig. 1b). The results demonstrated that after inducing atherosclerosis plaques, the GC group showed a significantly increased formation of aortic lesions (13·1 ± 2·4%) compared to the CON group (4·2 ± 1·2%) ($P < 0·001$). This increase was approximately 212% in the GC group, compared to that in the control group, suggesting that the induction of atherosclerosis using the GAN with -carnitine diet was highly efficient (Fig. 1c). Compared to the GC group, supplementation with low-dose GEO, high dose GEO, and citral substantially alleviated this effect by reducing the occurrence of aortic plaques by 23, 20, and 29%, respectively ($P = 0·0043$, $P = 0·0610$, $P = 0·0311$, respectively). We further examined the lipidaemic biomarkers, including the level of plasma

triglyceride, cholesterol, HDL, LDL, and ox-LDL (Fig. 1d-h). GC elevated the plasma cholesterol, HDL, and LDL levels ($P < 0{\cdot}0001$, $P = 0{\cdot}0008$, and $P < 0{\cdot}0001$, respectively), suggesting that this intervention considerably affected the circulation of lipids. However, there was no significant effect on the plasma triglyceride and ox-LDL levels. Trends for reduction in plasma cholesterol and LDL levels were found in ApoE$^{-/-}$ mice supplemented with GEO and citral. Moreover, high-dose GEO and citral increased the HDL levels ($P = 0{\cdot}0054$ and $P = 0{\cdot}0015$, respectively). These results demonstrated the beneficial effect of GEO and citral in preventing atherosclerosis lesion formation and improving the plasma lipid profile.

Improved glucose and insulin homeostasis, hepatic damage biomarkers, and reduced plasma pro-inflammatory cytokines

Further, we investigated the effect of GC, GEO, and citral on glucose and insulin homeostasis, hepatic damage biomarkers, and plasma pro-inflammatory cytokines. HFD feeding can result in glucose and insulin metabolism. This study found that GC significantly increased plasma glucose ($P = 0{\cdot}0048$) and insulin levels (Fig. 2a-b). We calculated HOMA-IR values to determine insulin resistance after administering different treatments. Similar to the plasma glucose and insulin data, the HOMA-IR value was substantially increased ($P = 0{\cdot}0554$) in the GC group (Fig. 2c). Low-dose GEO, high-dose GEO, and citral were found to be critical in improving plasma glucose ($P = 0{\cdot}0480$, $P = 0{\cdot}1733$, and $P = 0{\cdot}0007$, respectively), insulin ($P = 0{\cdot}0270$, $P = 0{\cdot}0298$, and $P = 0{\cdot}0163$, respectively), and HOMA-IR ($P = 0{\cdot}0113$, $P = 0{\cdot}0192$, and $P = 0{\cdot}0018$, respectively) levels. We also found that GC had a powerful impact on hepatic AST and ALT ($P < 0{\cdot}0001$ and $P = 0{\cdot}0319$), increasing their levels 2·2- and 3·4-fold, respectively, compared to those in the CON group (Fig. 2d-e). GEO and citral had no impact on AST levels; however, low-dose GEO, high-dose GEO, and citral substantially ameliorated the ALT levels ($P = 0{\cdot}1216$, $P = 0{\cdot}1789$, and $P = 0{\cdot}0491$, respectively). We further investigated whether GEO and citral can lower blood inflammation by measuring the plasma levels of pro-inflammatory cytokines. GC exhibited an adverse effect on systemic inflammation by increasing plasma TNF-α, IL-6, and IL-1β levels ($P < 0{\cdot}0001$, $P = 0{\cdot}0149$, and $P = 0{\cdot}0638$, respectively). Both low and high doses of GEO tended to lower TNF-α and IL-6 levels and substantially reduced IL-1β levels ($P = 0{\cdot}0413$ and $P = 0{\cdot}0835$, respectively). Moreover, citral exhibited a further enhanced substantial effect on reducing TNF-α, IL-6, and IL-1β levels ($P = 0{\cdot}0212$, $P = 0{\cdot}1014$, and $P = 0{\cdot}0520$, respectively). Thus, both GEO and citral have the potential to alleviate systemic inflammation, hepatic damage, and insulin resistance.

Remodelling of gut microbiota and suppression of metaorganismal -carnitine-TMAO metabolic pathway

TMAO is an atherosclerotic risk factor. The primary multistep metaorganismal (gut microbiota and host) pathway for TMAO production through carnitine metabolism is: -carnitine → γ-butyrobetaine (γBB) → TMA → TMAO.[21] Compared to the CON group, the GC group showed significantly increased plasma TMA,

TMAO, γ-BB, and carnitine levels (P = 0·0032, P = 0·0135, P < 0·0001, and P < 0·0001, respectively), accounting for a 11·2-, 4·1-, 43·3-, and 1·9-fold increase, respectively (Fig. 3a-d). Low and high doses of GEO and citral were capable of reducing plasma TMA and TMAO levels; low-dose and high-dose GEO, in particular, significantly reduced plasma TMAO levels (P = 0·0398 and P = 0·0202, respectively). For plasma γ-BB, a reduction trend was observed in the group treated with GEO, and the effect was more pronounced in the group treated with citral (P = 0·0663).

Since gut microbiota plays a critical role in the development of CVD and atherosclerosis, we aimed to elucidate the effect of GC, GEO, and citral on gut microbiota. To achieve this, we further examined the faeces microbiota composition using V3–V4 16S rRNA gene sequencing technique. The raw sequence data were processed using the QIIME2 pipeline to obtain the amplicon sequence variance (ASV) table. The processed ASVs were compared to taxonomic classification against the SILVA database (version 132). The QIIME2 platform generated 1504 ASVs assigned to 190 species and 122 genera. The vegan package in R was employed to calculate α-diversity, including observed species and Shannon diversity index. The GC group showed a significant reduction in the observed species (P = 0·0003) and tended to lower the Shannon diversity index, suggesting that the GAN/ -carnitine diet decreased the abundance of particular gut microbiome and hampered the evenness of the microbiota (Fig. 3e-f). GEO tended to elevate the Shannon diversity index, along with citral which increased it significantly (P = 0·0041).

We then computed β-diversity based on the Bray – Curtis distance (Fig. 3g). The results demonstrated that GC, GEO, and citral affected and remodelled the faecal microbiota. PCoA showed significant separation among all groups (ANOSIM: R = 0·6812, P < 0·001). The GC group showed a distinct separation from the CON group relying on the X-axis (PCoA1; 35·14%), suggesting that the GAN/ -carnitine diet was a primary factor in the alteration of faecal microbiota. GEO and citral also had a secondary impact on the gut microbiome. Citral and GEO locomoted the gut microbiome on the Y-axis in a dose-dependent manner (PCoA2; 12·77%). The dot of high-dose GEO-treated mice displayed an additional shift outward from the GC group, suggesting that a stronger dose exhibited a more considerable impact on the gut microbiome. The PCoA plot also provided information on the degree of aortic lesion, along with the TMA and TMAO levels. A larger circle represented a more severe aortic lesion while a deeper colour in the circle exhibited a higher level of TMA or TMAO—both characteristics displayed by the GC group as compared to the CON group. The GEO and citral-supplemented groups tended to reduce the circle's size and colour intensity. We also assessed the association between the genus and distance structure of each mouse's gut microbiome using the envfit function of the vegan R package. Vectors in the PCoA plot represented a significant genus (P < 0·001), and its length indicated the strength of association. The CON group correlated to beneficial genera such as *Lactobacillus*, *Alistipes*, *Bifidobacterium*, and other bacteria —the *Eubacterium xylanophilum group*, *Ruminococcaceae UCG − 014*, *Ruminococcaceae UCG − 013*, *Desulfovibrio*, *Candidatus Saccharimonas*, *Candidatus Stoquefichus*, *Turicibacter*, *Family XIII UCG − 001*, *Ruminiclostridium 5*, *Lachnospiraceae FCS020 group*, and *Clostridium sensu stricto 1*. The GC-treated group was associated with *Faecalibaculum*. A low dose of GEO was related to the beneficial mucin degrading genus *Akkermansia* and other bacteria such as *Enterococcus* and *Parasutterella*. The citral-supplemented group was associated with *Allobaculum* and *Dubosiella*—CVD negative correlated

microbiomes, *Coriobacteriaceae UCG − 002*, *Lachnoclostridium* and the *Eubacterium coprostanoligenes group*. Therefore, GEO and citral potentially re-shaped the gut microbiome and decreased the metaorganismal metabolism of -carnitine by both gut microbiota and host to form TMAO.

GEO and citral supplementation favourably modulated gut microbiota at the genus level

We further performed statistical analyses using the Kruskal–Wallis test; the genera that significantly differed among the five experimental groups ($P < 0{\cdot}05$) were selected and plotted as a heatmap (Fig. 4). The results demonstrated that there were 47 significantly different genera. The left panel displayed the hierarchical clustering of gut microbiota at the genus level divided into two major clusters indicating the differences between the CON group and GC-treated group. The data suggests that the form of diet (control diet or GAN diet with -carnitine) was the prime factor differentiating the faecal microbiota at genus level. The GC-treated group cluster consisted of 29 genera, whereas the control diet cluster consisted of 18. Supplementation of GEO and citral was found in the sub-cluster within the GC-treated cluster, suggesting that GEO and citral played a secondary role in altering gut microbiota. The top panel indicates the experimental group and degree of aortic lesion along with the TMA and TMAO levels, which exhibited increased values in the GC group but were reduced in the GEO and citral treated group. We also performed pairwise statistical analyses in the heatmap using an unpaired Wilcoxon signed-rank test displayed in the left panel with varying P-values.

Compared to the CON group, the GC group was enriched in CVD-related bacteria *Enterorhabdus*, *Romboutsia*, *Proteus*, the *Eubacterium nodatum group*, *Escherichia-Shigella*, and other genera—the *Eubacterium coprostanoligenes group*, *Parasutterella*, *Muribaculum*, and *Enterococcus*. The GC group showed depletion of several beneficial microbiotas, such as *Bifidobacterium* and *Alistipes*. These data suggested that the GAN diet with -carnitine caused an adverse effect on gut microbiota homeostasis by increasing CVD-associated microbiome but decreasing particular beneficial microbiome. We further examined the role of GEO and citral on faecal microbiota. There were 16 genera in low-dose GEO, 13 in high-dose GEO, and 13 in the citral groups significantly different than those in the GC group. Interestingly, GEO supplementation reduced the relative abundance of CVD-associated bacteria *Enterorhabdus* and *Proteus* but increased the beneficial bacteria, *Allobaculum*. Besides, citral also decreased the abundance of *Proteus* but increased *Allobaculum* and *Dubosiella*.

We further performed Spearman's correlation analysis to assess the relationship of the significant genus based on the heatmap with CVD-related biomarkers. The right panel shows Spearman's correlation analysis of the genus versus GC, aortic lesion, TMA, TMAO, GEO, and citral. Seven genera positively correlated with an aortic lesion, including the *Eubacterium coprostanoligenes group*, *Parasutterella*, *Enterohabdus*, *Akkermansia*, *Romboutsia, Proteus*, and *Olsenella*—a microbiome particularly associated with CVD. Fifteen genera were negatively correlated with aortic lesions, including the beneficial bacteria *Bifidobacterium* and *Alistipes*. Interestingly, CVD-related *Enterohabdus* positively correlated with plasma TMAO levels. GEO was positively associated with a healthy microbiome consisting of *Akkermansia*,

whereas citral positively correlated with *Allobaculum* and *Dubosiella*. In summary, the heatmap and correlation data indicated that GC adversely affected gut microbiota, resulting in microbiota dysbiosis. However, GEO and citral exhibited a favourable effect and improved the general gut microbiota composition. Therefore, GEO and citral supplementation in the GC ApoE$^{-/-}$ mouse model may restore gut microbiota and its metabolites as well as ameliorate atherosclerosis.

Discussion

This study demonstrated that GEO and citral can potentially ameliorate atherosclerosis by suppressing metaorganismal metabolism of gut microbiota-host-derived TMA and TMAO, favourably remodelling the gut microbiota composition in ApoE$^{-/-}$ treated mice administered with a GAN and -carnitine diet. This diet mimics the Western style diet, with habitual red meat consumption. In addition, GEO and citral supplementation significantly lowered plasma IL-1β, TNF-α, glucose, and insulin levels. Ginger possesses cardioprotective,[22] anti-inflammatory,[19] anti-microbial,[23] and glucose-modulating functions.[20] Dietary ginger extract suppresses the TMAO-aggravated elevation of plasma cholesterol in mice and improves the anti-inflammatory response by reducing TNF-α, IL-1β, and IL-6 levels.[18] However, previous studies have not reported whether GEO and citral improve atherosclerosis by modulating gut microbiota composition. Hence, this study aimed to elucidate the underlying mechanisms of GEO and citral on the gut microbiota-CVD axis.

Hyperlipidaemia is the most crucial risk factor for atherosclerosis, which is the primary cause of CVD.[24] This study showed that GC increased total cholesterol, LDL, and HDL levels, primarily due to the GAN diet, which contained 2% cholesterol. The GAN diet comprises 40 kcal% of fat, mainly from palm oil. The intake of palm oil-containing HFD elevates blood cholesterol, LDL, and HDL levels.[14, 15] GEO and citral administration did not decrease the total plasma cholesterol and LDL levels but increased the HDL levels, suggesting their beneficial effect on improving blood lipid profile. In addition, GC increased plasma glucose, insulin, and HOMA-IR levels, suggesting its potential in inducing the metabolic syndrome, which was consistent with the findings of previous studies.[14, 15] Our data demonstrated that GEO and citral significantly improved glucose tolerance and insulin resistance, with a potential to improve glucose homeostasis. This study found no significant difference in blood triglyceride levels after receiving GC intervention with/without GEO and citral supplementation. Since the triglyceride and cholesterol content in HFD is high, excessive cholesterol intake downregulates the production of cholesterol esters and lipoproteins in the liver, thereby inhibiting the production of triglycerides in the liver.[14] Besides, the GAN diet has less impact on the total plasma glyceride levels.[13]

Atherosclerosis is a chronic inflammatory disease commonly manifesting as increased circulating pro-inflammatory cytokines.[25] We observed the elevation of pro-inflammatory cytokine TNF-α levels and rising trends in plasma IL-1β and IL-6 levels in GC-treated ApoE$^{-/-}$ mice. IL-1β$^{-/-}$/ApoE$^{-/-}$ mice or TNF-α$^{-/-}$/ApoE$^{-/-}$ mice enhance inflammation and reduce aortic lesions, indicating the importance of IL-1β and TNF-α on aortic lesion development.[26, 27] In addition, palm oil in concert with high cholesterol enhances

the production of IL-1β, causing inflammation.[28] In our research, GEO and citral supplementation exhibited immunomodulatory activity by reducing plasma IL-1β and TNF-α levels, respectively.

Consuming an unhealthy diet is associated with the development of CVD through traditional pathways–hyperlipidaemia and chronic inflammation as well as the metaorganism-pathogenesis pathway involving gut microbiota, its metabolites, and the metabolic pathway of the host.[3] As reported earlier, food nutrients such as -carnitine can be metabolized through a specific gut microbiome to form γBB and TMA.[21] TMA can be subsequently oxidized to the CVD risk factor TMAO by the host hepatic flavin monooxygenase.[6] This study found that the plasma concentrations of carnitine, γ-BB, TMA, and TMAO in the GC group were significantly elevated. In contrast, γBB was not detected in the CON group, suggesting that these metabolites are produced by the gut microbiota using -carnitine as a substrate. Apart from supplementation with -carnitine, high-fat and high-sugar diets significantly increase blood TMAO concentrations in mice.[9, 12] The previous study induced a similar concentration of -carnitine but without using the HFD; this approach produced approximately 20 μM of blood TMAO.[17] Our results demonstrated that a combination of the GAN diet and -carnitine exhibited an enhanced potential to promote the production of blood TMAO (approximately 50 μM). In this study, GEO and citral supplementation significantly reduced the production of plasma TMA and TMAO, indicating that they may possess antibiotic-like activity, suppressing the production of TMA-related bacteria in the gut. Moreover, GEO and citral functioned as anti-inflammatory agents to reduce the levels of circulating inflammatory markers, thus ameliorating atherosclerosis.

A previous study investigated the effect of HFD on the gut microbiota composition in mice. The results demonstrated a change in gut microbiota after two weeks of HFD.[14] In another study, mice were fed a palm oil-containing HFD, and it was found that the GAN diet induced obesogenic and metabolic changes, NASH phenotype, altered gut microbiota composition and function, increased gut dysbiosis, reduced beneficial microbiota, and increased pathogenic bacteria, intestinal leakage, as well as endotoxemia.[13] This study found that, compared to the control group, the GC group modified the - and β-diversity of faecal microbiota. It showed an increase in CVD-related bacteria *Enterorhabdus*, *Romboutsia*, *Proteus*, the *Eubacterium nodatum group*, and *Escherichia-Shigella* but reduced specific beneficial microbiomes, such as *Bifidobacterium* and *Alistipes*. Spearman's correlation analysis revealed seven genera positively correlated with an aortic lesion, including the *Eubacterium coprostanoligenes group*, *Parasutterella*, *Enterohabdus*, *Akkermansia*, *Romboutsia*, *Proteus*, and *Olsenella*. In addition, *Bifidobacterium* and *Alistipes* negatively correlated with aortic lesions. Interestingly, *Enterohabdus* is positively associated with plasma TMAO levels.

A previous study found that HFD-induced ApoE$^{-/-}$ mice has a higher relative abundance of *Enterorhabdus*.[29] *Romboutsia* is more abundant in the normal blood pressure group than in patients with hypertension.[30] It is also one of the indicators of systolic blood pressure.[31] *Proteus penneri* and *Escherichia fergusonii* are well-known CVD-related bacteria that can convert -carnitine to γBB.[32] Particularly, the *Eubacterium nodatum group* and *Emergencia timonensis* can anaerobically metabolize γ-

BB to TMA.[21] In contrast, probiotics such as *Bifidobacterium breve* and *Bifidobacterium longum* exhibit cardiometabolic protection by modulating the gut microbiota and reducing plasma TMAO level in choline-fed mice.[33] *Alistipes*, short-chain fatty acid (SCFA)-producing bacteria, were enriched in healthy volunteers compared to NASH patients. They could play a beneficial role against liver disease by secreting SCFA, which helps in the alleviation of several diseases. However, *Alistipes* are associated with hypertension.[34] Accordingly, the GAN diet with -carnitine may unfavourably affect the gut microbiota composition, causing microbiota dysbiosis.

In this study, GEO and citral modified the gut microbiota - and β-diversity indices. Interestingly, GEO feeding decreased the abundance of the CVD-associated bacteria *Enterorhabdus* and *Proteus* but increased the abundance of the beneficial bacteria *Allobaculum*. Furthermore, citral also lowered the abundance of *Proteus* and enriched *Allobaculum* and *Dubosiella*. GEO positively correlated with *Akkermansia*, whereas citral was positively associated with *Allobaculum* and *Dubosiella*.

Akkermansia muciniphila prevents atherosclerosis in ApoE$^{-/-}$ mice by decreasing endotoxemia and inflammation.[35] Additionally, ginger extract increases the relative abundance of *Allobaculum* in HFD-induced mice. Faecal microbiota transplantation from the HFD with ginger extract supplementation indicates an increased occurrence of *Allobaculum*.[36] In addition, the abundance of *Allobaculum* is lower in HFD-induced ApoE$^{-/-}$ mice, implying that it is negatively correlated with atherosclerosis.[37] *Dubosiella* has a decreased abundance in hypertensive mice induced by a high salt diet, which negatively correlates with CVD.[38] GEO remodels the gut microbiota and reverses dysbiosis to achieve NASH amelioration in the GAN diet with LPS-injected murine NASH model; moreover, GEO suppresses the NLRP3 inflammasome and mediates the gut microbiota-LPS-TLR4 pathway.[20] Collectively, GEO and citral showed potential advantages by improving the gut microbiota composition in the GC ApoE$^{-/-}$ mouse model.

In summary, our study demonstrated that GEO and citral exhibit cardio-protective effects by modulating gut microbiota, inhibiting the formation of TMAO, reducing pro-inflammatory cytokine levels, and improving insulin resistance (Fig. 5). Thus, GEO and citral may serve as potential dietary supplements for CVD prevention.

Methods

GEO extraction and analysis of its major components

Ginger (*Zingiber officinale* Roscoe) samples were purchased from Nantou Mingjian Country Farmers Association, Nantou, Taiwan. They were washed, cut into slices, and blended with three volumes of distilled water. GEO was then extracted from the resulting puree using steam distillation for approximately six hours, yielding a yellowish clear essential oil. The extract concentration was approximately 0·14% (w/w). Its chemical constitution was analysed using Thermo Scientific Focus gas chromatography, equipped with an AI 3000 II autosampler and a flame ionization detector. The analysis

program and conditions are as follows: flow rate of the carrier N_2 gas was 1 mL/min with a split ratio of 40:1; initial column temperature, 50 ℃; final column temperature, 200 ℃; an increase of 7 ℃/min to 200 ℃ held for 0 min; injector temperature, 250 ℃; detector temperature, 250 ℃, and injection volume, 0·3 µL. Citral (purity > 95%, Sigma-Aldrich, USA) was used as a standard. A representative chromatogram is shown in Supplementary Fig. 1. The primary component of GEO was citral, comprised of a mixture of the two geometric isomers, geranial and neral. The retention times of geranial and neral were 17·04 min and 17·82 min, respectively. The area under curve (AUC) was calculated to quantify the amount of both components in GEO. In this study, citral accounted for approximately 31% (neral: 18·8% and geranial: 12·2%), which was similar to that obtained in our previous study (30%).[19]

Animal model

The ApoE$^{-/-}$ mice were originally purchased from the Jackson Laboratory (Bar Harbor, ME) and bred in our animal house. The animals were handled according to the guidelines established by the Institutional Animal Care and Use Committee of National Taiwan University (Approval No: NTU-109-EL-00131). Eight-week-old C57BL/6 ApoE$^{-/-}$ female mice were housed in a room at 22 ± 2°C with a 12 h light/dark cycle. Compared to male ApoE$^{-/-}$ mice, female ApoE$^{-/-}$ mice exhibited pronounced flavin monooxygenase 3 (FMO3) activity and significantly elevated plasma TMAO levels; hence, the female mice were selected for this study.[39] After adaptation for two-weeks, the mice were randomly divided into five groups with eight mice in each: (1) CON (control diet); (2) GC (Gubra Amylin NASH diet [GAN diet] + -carnitine in water [1·3%]); (3) GC + GEO_{Low} (GC + Ginger essential oil (GEO) [50 mg/kg bw/day]); (4) GC + GEO_{High} (GC + GEO [100 mg/kg bw/day]); (5) GC + CIT (GC + Citral [20 mg/kg bw/day]). The control diet contained 10 kcal% fat (Research Diets, Inc., NJ, USA; D12450K), while the GAN diet contained 40 kcal% fat, 20 kcal% fructose, and 2% cholesterol (GAN diet; Research Diets, Inc., NJ, USA; D09100310).[14] GEO and citral were dissolved in soybean oil. All mice were fed the experimental diets and liquid *ad libitum*. After 16 weeks, the mice were sacrificed using carbon dioxide asphyxiation and blood was collected by cardiac puncture through a syringe.

Oil red staining of the aorta

The aorta of the mice was rinsed with phosphate-buffered saline to clean residual blood and dissected under the microscope using a microscissor and tweezers, to remove the fatty tissue surrounding it. The dissected sample was then fixed on a plate and soaked in 10% formalin overnight. Further, it was washed with distilled water for 5 min, soaked twice in propylene glycol for another 5 min, stained with oil red for approximately 10 min, soaked in 85% propylene glycol for 3 min, and washed again with distilled water for 3 min. An image of the stained aorta was captured under the microscope and the aortic lesions were quantified using the Image J software (Version 1.8.0).[17]

Plasma biochemistry analyses

Blood samples from the mice were centrifuged at 1000 × *g* for 15 min (4°C) to extract plasma. The plasma samples were then analysed for total cholesterol, total triglyceride, high-density lipoprotein (HDL),

glucose, aspartate aminotransferase (AST), and alanine aminotransferase (ALT) levels using commercial test strips in an automatic blood analyser (SpotchemTM II reagent strip; Arkray Inc., Kyoto, Japan).[17] Oxidized low-density lipoprotein (ox-LDL) was measured using a commercial enzyme-linked immunosorbent assay (ELISA) kit (CSB-E07933m, Cusabio Biotech Co., Ltd., China)

Measuring plasma concentrations of TMA, TMAO, γBB, and carnitine using liquid chromatography-mass spectrometry

For plasma sample preparation, 5 μL of plasma was mixed with 20 μL of deionized water; 10 μL of this mixture was then added to 190 μL of isotopically labelled internal standards (d_3-carnitine, $^{13}C_3$-TMA, and $^{13}C_3$-TMAO) in 0·1% formic acid acetonitrile solution. The solution was subsequently centrifuged at 12,000 × *g* for 5 min (4°C), and the supernatant was separated. Subsequently, 100 μL of this supernatant was used for the quantification of TMA, TMAO, γBB, and carnitine levels using liquid chromatography-tandem mass spectrometry (LC-MS/MS; EXION LC, ABSCIEX with TripleQuad 5500, ABSCIEX).

For LC-MS/MS analysis, 5 μL of each plasma was injected into an ABSCIEX EXION LC system coupled with an ABSCIEX TripleQuad 5500 mass spectrometer (AB SCIEX, Canada). The separation was performed using an ACQUITY UPLC BEH Amide Column (2·1 × 150 mm, 1·7 μm, Waters, USA) maintained at 40°C. Mobile phase A was 0·1% formic acid in deionized water, and mobile phase B was 0·1% formic acid in acetonitrile; flow rate was 0·15 mL/min. The LC program was as follows: 0–1 min, 50% solvent B; 1–2 min, 50–40% solvent B; 2–3 min, 40–50% solvent B; and 3–5 min, 50% solvent B. The electrospray was set in positive ionization mode with the following parameters: curtain gas supply, 50 psi; capillary temperature, 500°C; spray voltage rating, 5 kV. The concentration of each analyte was calculated from calibration curves relating the peak area ratio to its corresponding standard.[17]

Assessment of insulin resistance

Plasma insulin levels were measured using a commercial ELISA kit (Mercodia mouse insulin ELISA kit), according to the manufacturer's instructions (10-1247-01, Mercodia Inc, USA). The Homeostatic Model Assessment-Insulin Resistance index (HOMA-IR) was calculated using the following formula: fasting plasma glucose levels (mmol/L) × fasting plasma insulin levels (mU/L) / 22·5.[40]

Analysis of pro-inflammatory cytokine content in plasma

The level of pro-inflammatory cytokines, tumour necrosis factor alpha (TNF-α), interleukin (IL)1-β, and IL-6 in plasma was measured using a commercial ELISA kit (Invitrogen, USA), according to the manufacturer's instructions.[19]

Gut microbiota composition analysis

Mouse faecal samples were collected from the large intestine, snap frozen in liquid nitrogen, and stored at -80 ℃ before use. Faecal samples were used for DNA extraction, V3-V4 region 16S rRNA gene amplification, and construction of the sequencing library. Faecal genomic DNA was extracted using the

QIAamp Power Faecal Pro DNA Kit (QIAGEN, Netherlands), according to the manufacturer's instructions. The V3-V4 region of the 16S rRNA gene was amplified using the forward and reverses primer pairs [(Forward = 5'-TCG TCG GCA GCG TCA GAT GTG TAT AAG AGA CAG CCT ACG GGN GGC WGC AG-3') and (Reverse = 5'-GTC TCG TGG GCT CGG AGA TGT GTA TAA GAG ACA GGA CTA CHV GGG TAT CTA ATC C-3')]. The polymerase chain reaction included an initial step of 95°C for 3 min, followed by 25 cycles of 95°C for 30 s, 55°C for 30 s, 72°C for 30 s, and a final extension of 72°C for 5 min. The final amplified products were subsequently visualized using 2% agarose gel electrophoresis. The sequencing library was constructed using the Illumina MiSeq platform, according to manufacturer's instructions. The raw sequences were processed according to the QIIME2 pipeline, and the amplicon sequence variant (ASV) table was prepared according to the SILVA database (version 132). The vegan package in R was employed to calculate the α-diversity, including observed species and the Shannon diversity index. Principal coordinates analysis (PCoA) was presented as beta diversity, and it was performed using the Bray-Curtis distance. The analysis of similarity (ANOSIM) was calculated to determine heterogeneity of the faecal microbiota among all groups. Heatmap and correlation were plotted using the heatmap3 and corrplot packages in R, respectively.[17]

Statistical analyses

Data are represented as the mean ± standard deviation (SD). An unpaired two-tailed Student's t-test or one-way analysis of variance (ANOVA) with Tukey's range test was used to compare the group means. Wilcoxon signed-rank test, Kruskal–Wallis test, Dunn's multiple comparison test, unpaired two-tailed Student's t-test, and one-way ANOVA with Tukey's range test were used to analyse the faecal microbiome data set based on whether the datasets were normally distributed. All statistics were analysed using the Graphpad Prism (version 9.4.1) or R (version 3.6.1).

Declarations

DATA AVAILABILITY

The raw 16S rRNA sequencing data used to produce all figures are accessible at the NCBI Short Read Archive under the following accession numbers: BioProject: PRJNA894809, BioSample: SAMN31475470, and SRA: SRR22062157-78.

CODE AVAILABILITY

Bioinformatic tools, software version, parameters, and open-source code used in this present study are described in the "Methods" section. More details regarding the code to reproduce the analyses are available upon request.

ACKNOWLEDGEMENTS

This study was supported by the Ministry of Science and Technology, Taiwan (109-2327-B-002-005, 109-2314-B-002-103-MY3, 109-2314-B-002-064-MY3, 110-2327-B-002-007, 111-2628-B-002-047, and 111-

2327-B-002-008). The authors would also like to acknowledge the technical research services for mass spectrometry provided by the National Taiwan University (NTU) Consortia of Key Technologies.

COMPETING INTERESTS

The authors declare that there are no competing interests.

AUTHOR CONTRIBUTIONS

S.P. provided instructions and assisted in the experiment, performed the bioinformatic and statistical analysis, interpreted the results and drafted the manuscript. W.K.W. designed and provided instructions for the experiments, along with reviewing and revising the manuscript. S.Y.P. performed the animal experiments. Y.J.T. and Y.C.H. assisted in all experiments. R.A.C., H.S.H., and Y.H.C. supervised all the experiments. H.L.C. and K.C.Y. provided technical support in the ApoE$^{-/-}$ experiment. C.C.H. oversaw the target metabolomics analysis and assisted in the mass spectrometry analysis. T.C.D.S. and C.T.H. critically reviewed the manuscript. M.S.W. and L.Y.S. designed the experiments, provided funding for the study, and revised the manuscript. All authors had full access to all the data in the study and accept responsibility to submit for publication.

References

1. Roth, G.A. et al. Global, regional, and national burden of cardiovascular diseases for 10 causes, 1990 to 2015. J Am Coll Cardiol **70**, 1–25 (2017).
2. Ignarro, L.J., Balestrieri, M.L. & Napoli, C. Nutrition, physical activity, and cardiovascular disease: an update. Cardiovasc Res **73**, 326–340 (2007).
3. Panyod, S. et al. Modulation of gut microbiota by foods and herbs to prevent cardiovascular diseases. J Tradit Complement Med (2021).
4. Zhong, V.W. et al. Protein foods from animal sources, incident cardiovascular disease and all-cause mortality: a substitution analysis. Int J Epidemiol **50**, 223–233 (2021).
5. Simo, C. & Garcia-Canas, V. Dietary bioactive ingredients to modulate the gut microbiota-derived metabolite TMAO. New opportunities for functional food development. Food Funct **11**, 6745–6776 (2020).
6. Koeth, R.A. et al. Intestinal microbiota metabolism of L-carnitine, a nutrient in red meat, promotes atherosclerosis. Nat Med **19**, 576–585 (2013).
7. Senthong, V. et al. Intestinal microbiota-generated metabolite trimethylamine-N-oxide and 5-year mortality risk in stable coronary artery disease: the contributory role of intestinal microbiota in a COURAGE-like patient cohort. J Am Heart Assoc **5** (2016).
8. Zhu, W. et al. Gut microbial metabolite TMAO enhances platelet hyperreactivity and thrombosis risk. Cell **165**, 111–124 (2016).

9. Sun, G. et al. Gut microbial metabolite TMAO contributes to renal dysfunction in a mouse model of diet-induced obesity. Biochem Biophys Res Commun **493**, 964–970 (2017).
10. Chen, M.L. et al. Trimethylamine-N-oxide induces vascular inflammation by activating the NLRP3 inflammasome through the SIRT3-SOD2-mtROS signaling pathway. J Am Heart Assoc **6** (2017).
11. Bakhtiyari, M. et al. Contribution of obesity and cardiometabolic risk factors in developing cardiovascular disease: a population-based cohort study. Sci Rep **12**, 1544 (2022).
12. Chen, K., Zheng, X., Feng, M., Li, D. & Zhang, H. Gut microbiota-dependent metabolite trimethylamine N-oxide contributes to cardiac dysfunction in western diet-induced obese mice. Front Physiol **8**, 139 (2017).
13. Sheen, L.-Y. et al. Establishment of animal models for NASH and utilization for mining associated gut microbiota. Preprint at https://www.researchsquare.com/article/rs-1826044/v1 (2022).
14. Boland, M.L. et al. Towards a standard diet-induced and biopsy-confirmed mouse model of non-alcoholic steatohepatitis: Impact of dietary fat source. World J Gastroenterol **25**, 4904–4920 (2019).
15. Hansen, H.H. et al. Human translatability of the GAN diet-induced obese mouse model of non-alcoholic steatohepatitis. BMC Gastroenterol **20**, 210 (2020).
16. Lo Sasso, G. et al. The Apoe(-/-) mouse model: a suitable model to study cardiovascular and respiratory diseases in the context of cigarette smoke exposure and harm reduction. J Transl Med **14**, 146 (2016).
17. Panyod, S. et al. Atherosclerosis amelioration by allicin in raw garlic through gut microbiota and trimethylamine-N-oxide modulation. Npj Biofilms Microbi **8** (2022).
18. He, Z.Y. et al. Ginger attenuates trimethylamine-N-oxide (TMAO)-exacerbated disturbance in cholesterol metabolism and vascular inflammation. J Funct Foods **52**, 25–33 (2019).
19. Lai, Y.S. et al. Ginger essential oil ameliorates hepatic injury and lipid accumulation in high fat diet-induced nonalcoholic fatty liver disease. J Agric Food Chem **64**, 2062–2071 (2016).
20. Sheen, L.Y. Ginger essential oil prevents NASH progression by blockading the NLRP3 inflammasome and remodeling the gut microbiota-LPS-TLR4 pathway. Preprint at https://www.researchsquare.com/article/rs-1814299/v1 (2022).
21. Koeth, R.A. et al. l-Carnitine in omnivorous diets induces an atherogenic gut microbial pathway in humans. J Clin Invest **129**, 373–387 (2019).
22. Fuhrman, B., Rosenblat, M., Hayek, T., Coleman, R. & Aviram, M. Ginger extract consumption reduces plasma cholesterol, inhibits LDL oxidation and attenuates development of atherosclerosis in atherosclerotic, apolipoprotein E-deficient mice. J Nutr **130**, 1124–1131 (2000).
23. Wang, X. et al. Antibacterial activity and mechanism of ginger essential oil against *Escherichia coli* and *Staphylococcus aureus*. Molecules **25** (2020).
24. Nelson, R.H. Hyperlipidemia as a risk factor for cardiovascular disease. Primary Care **40**, 195–211 (2013).

25. Kobiyama, K. & Ley, K. Atherosclerosis a chronic inflammatory disease with an autoimmune component. Circ Res **123**, 1118–1120 (2018).
26. Kirii, H. et al. Lack of interleukin-1beta decreases the severity of atherosclerosis in ApoE-deficient mice. Arterioscler Thromb Vasc Biol **23**, 656–660 (2003).
27. Ohta, H. et al. Disruption of tumor necrosis factor-alpha gene diminishes the development of atherosclerosis in ApoE-deficient mice. Atherosclerosis **180**, 11–17 (2005).
28. Chang, P.Y., Chang, S.F., Chang, T.Y., Su, H.M. & Lu, S.C. Synergistic effects of electronegative-LDL- and palmitic-acid-triggered IL-1beta production in macrophages via LOX-1- and voltage-gated-potassium-channel-dependent pathways. J Nutr Biochem **97**, 108767 (2021).
29. Meng, Q.H. et al. The gut microbiota during the progression of atherosclerosis in the perimenopausal period shows specific compositional changes and significant correlations with circulating lipid metabolites. Gut Microbes **13**, 1–27 (2021).
30. Dan, X. et al. Differential analysis of hypertension-associated intestinal microbiota. Int J Med Sci **18**, 3748–3748 (2021).
31. Verhaar, B. et al. Associations between gut microbiome, short chain fatty acids and blood pressure across ethnic groups: the HELIUS study. Eur Heart J **41**, 2701–2701 (2020).
32. Romano, K.A., Vivas, E.I., Amador-Noguez, D. & Rey, F.E. Intestinal microbiota composition modulates choline bioavailability from diet and accumulation of the proatherogenic metabolite trimethylamine-N-oxide. mBio **6**, e02481 (2015).
33. Wang, Q. et al. *Bifidobacterium breve* and *Bifidobacterium longum* attenuate choline-induced plasma trimethylamine N-oxide production by modulating gut microbiota in mice. Nutrients **14** (2022).
34. Parker, B.J., Wearsch, P.A., Veloo, A.C.M. & Rodriguez-Palacios, A. The genus *Alistipes*: gut bacteria with emerging implications to inflammation, cancer, and mental health. Front Immunol **11**, 906 (2020).
35. Li, J., Lin, S., Vanhoutte, P.M., Woo, C.W. & Xu, A. *Akkermansia Muciniphila* protects against atherosclerosis by preventing metabolic endotoxemia-induced inflammation in $Apoe^{-/-}$ mice. Circulation **133**, 2434–2446 (2016).
36. Wang, J., Wang, P., Li, D.T., Hu, X.S. & Chen, F. Beneficial effects of ginger on prevention of obesity through modulation of gut microbiota in mice. Eur J Nutr **59**, 699–718 (2020).
37. Wu, M. et al. Effect of berberine on atherosclerosis and gut microbiota modulation and their correlation in high-fat diet-fed $apoe^{-/-}$ mice. Front Pharmacol **11**, 223 (2020).
38. Liu, T.H. et al. Gut microbiota-related evidence provides new insights into the association between activating transcription factor 4 and development of salt-induced hypertension in mice. Front Cell Dev Biol **8** (2020).
39. Bennett, B.J. et al. Trimethylamine-N-oxide, a metabolite associated with atherosclerosis, exhibits complex genetic and dietary regulation. Cell Metabolism **17**, 49–60 (2013).

40. Chen, R.A. et al. Dietary exposure to antibiotic residues facilitates metabolic disorder by altering the gut microbiota and bile acid composition. mSystems **7**, e0017222 (2022).

Figures

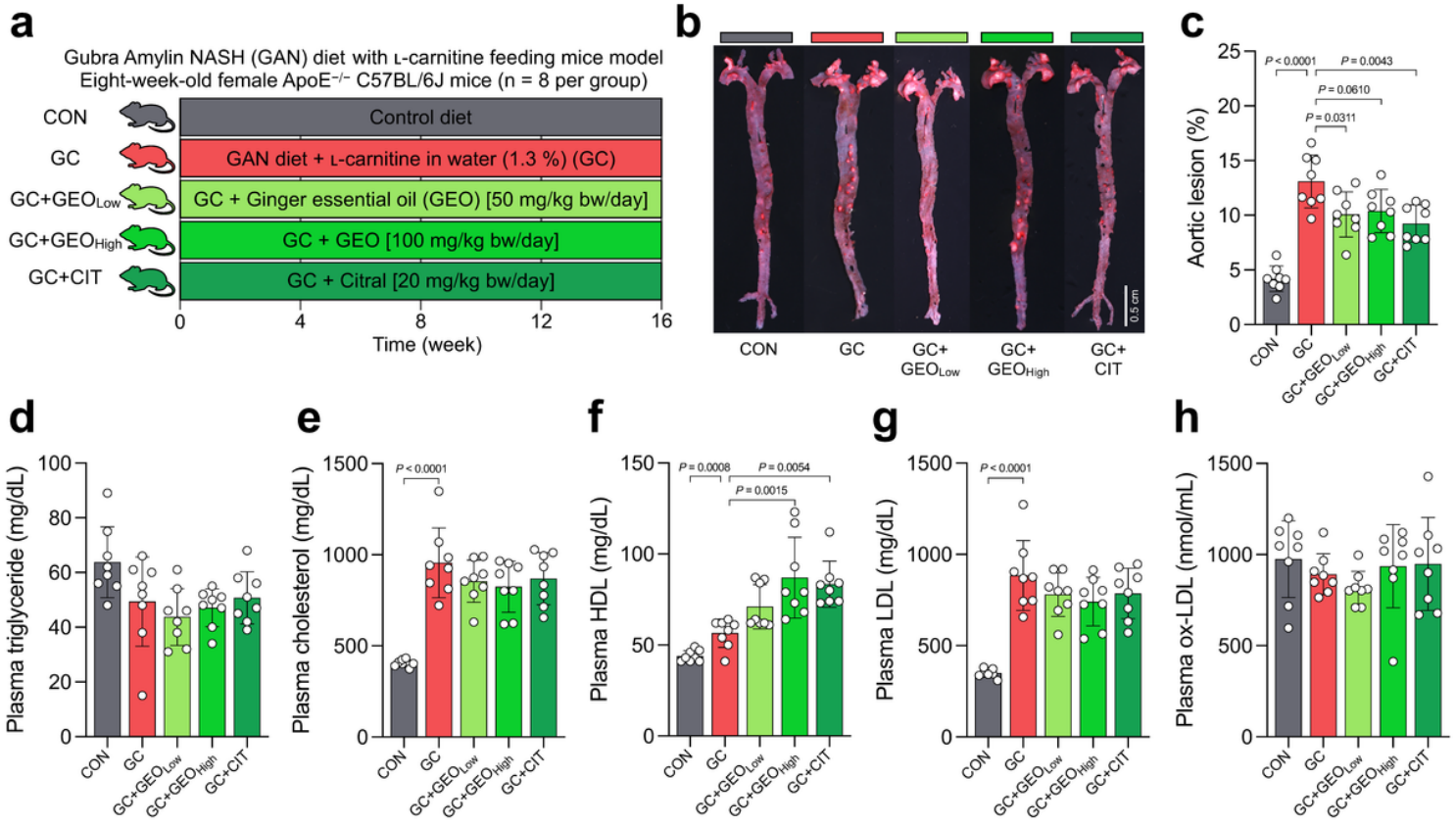

Figure 1

GEO and citral reduced aortic lesions and affected plasma lipid biomarkers in the GC-induced atherosclerosis female ApoE$^{-/-}$ mice (n = 8 per group). (a) experimental design; (b) representative image of oil red O stained aorta; (c) percentage of aortic lesions; levels of (d) plasma triglyceride; (e) total cholesterol; (f) high-density lipoprotein (HDL); (g) low-density lipoprotein (LDL); (h) oxidized LDL (ox-LDL). Dot plots are expressed as the mean ± standard deviation (SD). Statistical analyses were performed using an unpaired two-tailed Student's *t*-test, CON vs. GC groups; one-way analysis of variance (ANOVA) with Tukey's range test for comparing GC, GC + GEO$_{Low}$, GC + GEO$_{High}$, and GC + citral (CIT). GC: GAN with -carnitine diet, GEO: ginger essential oil

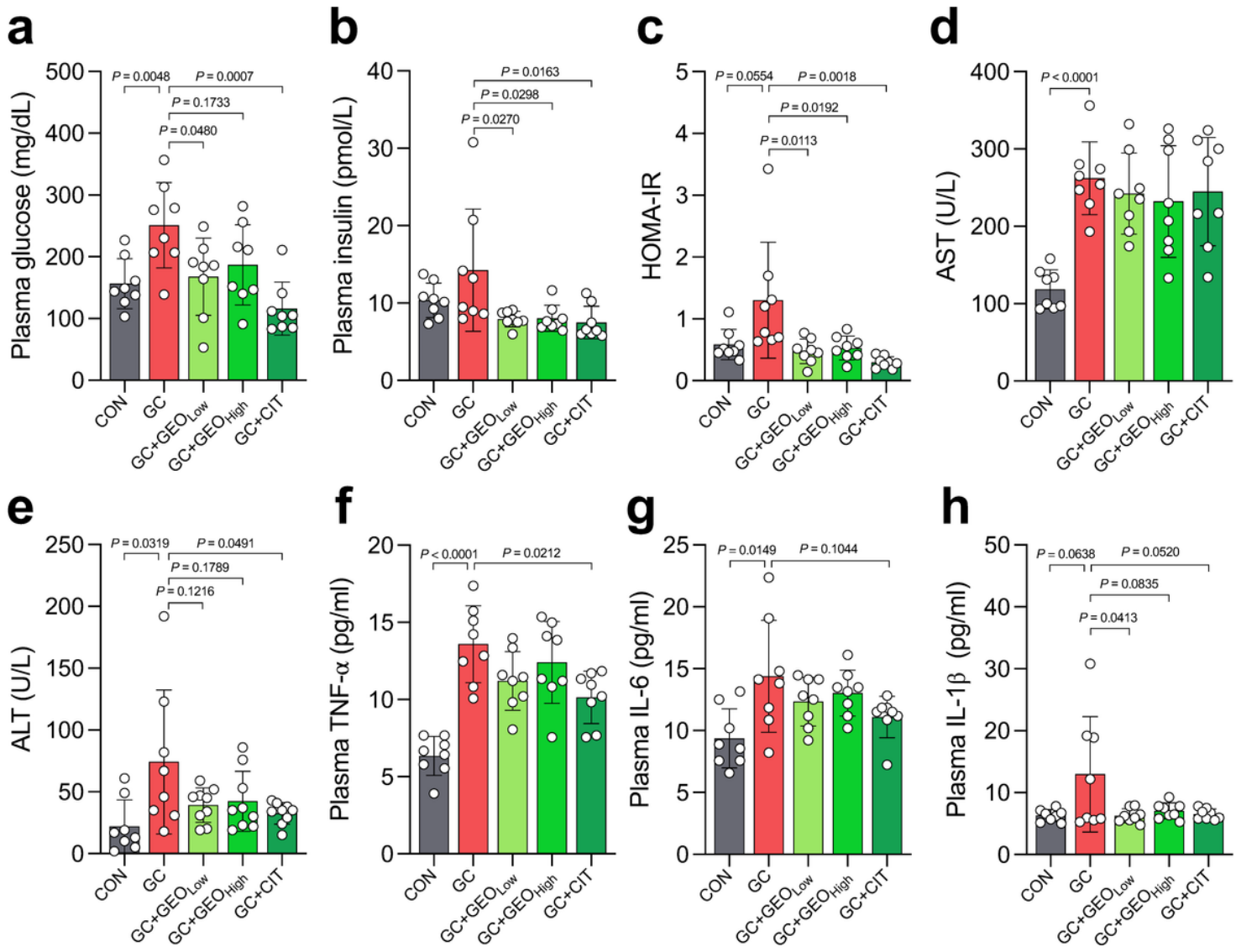

Figure 2

GEO and citral improved glucose homeostasis and plasma hepatic damage biomarkers and alleviated systemic inflammation in the GC-induced atherosclerosis female ApoE$^{-/-}$ mice (n = 8 per group). Levels of (a) plasma glucose; (b) insulin; (c) homeostasis model assessment for insulin resistance (HOMA-IR); (d) aspartate aminotransferase (AST); (e) alanine aminotransferase (ALT); (f) tumour necrosis factor-α (TNF-α); (g) interleukin 6 (IL-6); and (h) interleukin-1β (IL-1β). Dot plots are expressed as the mean ± SD. Statistical analyses were performed using an unpaired two-tailed Student's *t*-test, CON vs. GC groups; one-way ANOVA with Tukey's range test for comparing GC, GC + GEO_{Low}, GC + GEO_{High}, and GC + CIT. GC: GAN with -carnitine diet, GEO: ginger essential oil

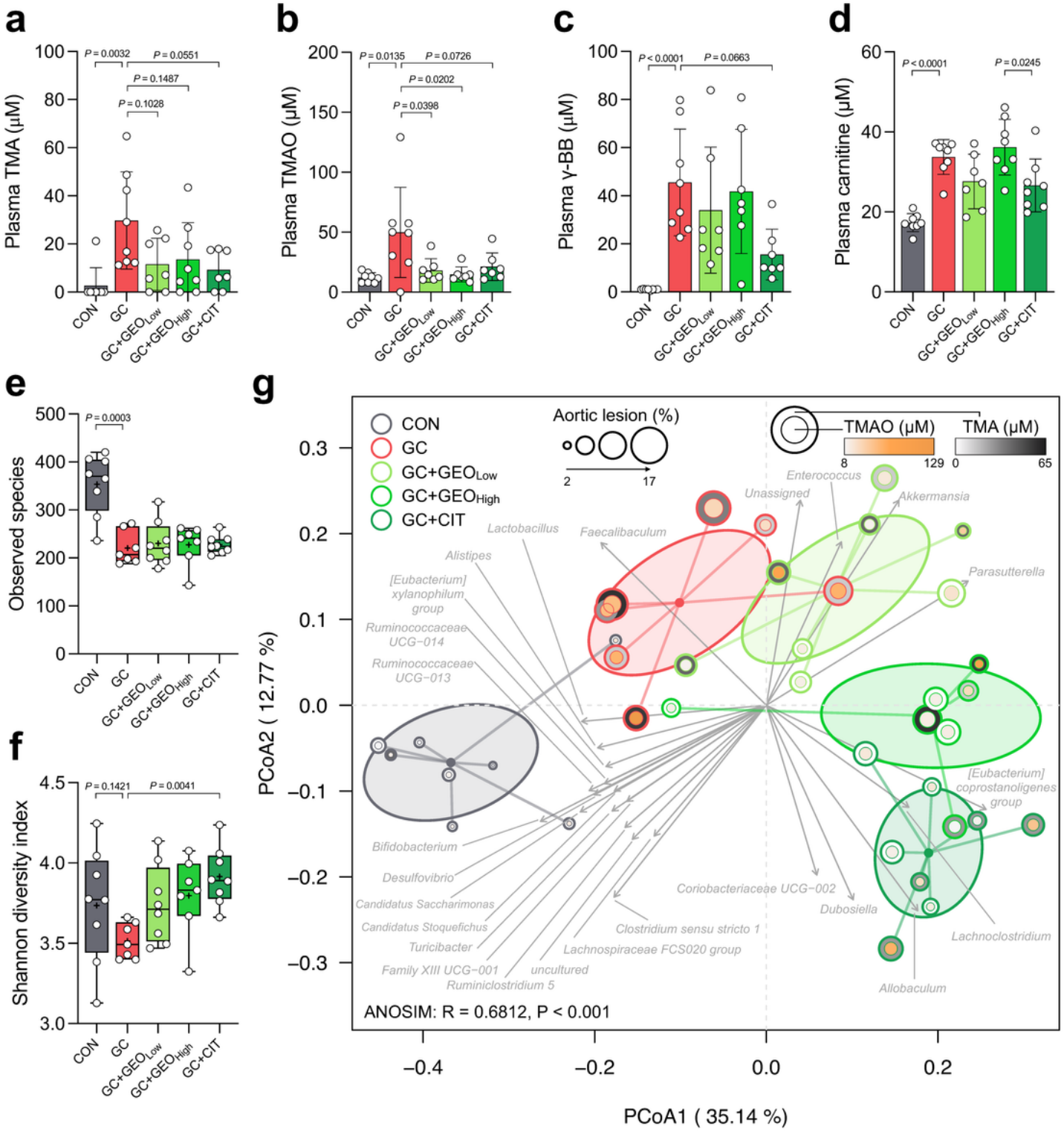

Figure 3

GEO and citral suppressed gut microbiota metabolites TMA and TMAO and remodelled gut microbiota composition in the GC-induced atherosclerosis female ApoE$^{-/-}$ mice. Levels of (a) plasma TMA, (b) TMAO, (c) γ-butyrobetaine (γ-BB), and (d) carnitine; (e) observed species; (f) Shannon diversity index; (g) principal coordinate analysis (PCoA) plot based on Bray–Curtis dissimilarity with gut microbiota-associated vector (n=7–8). Dot plots are expressed as the mean ± SD. Statistical analyses were

performed using an unpaired two-tailed Student's *t*-test CON vs. GC groups; one-way ANOVA with Tukey's range test for comparing GC, GC + GEO_{Low}, GC + GEO_{High}, and GC + CIT (Citral). ANOVA using distance matrices (Adonis) was calculated to determine heterogeneity of the faecal microbiota among the groups in PCoA. Vectors in the PCoA plot indicated a significant genus (P < 0.001), and its length shows the strength of the correlation. GC: GAN with -carnitine diet, GEO: ginger essential oil, TMA: trimethylamine, TMAO: trimethylamine-N-oxide

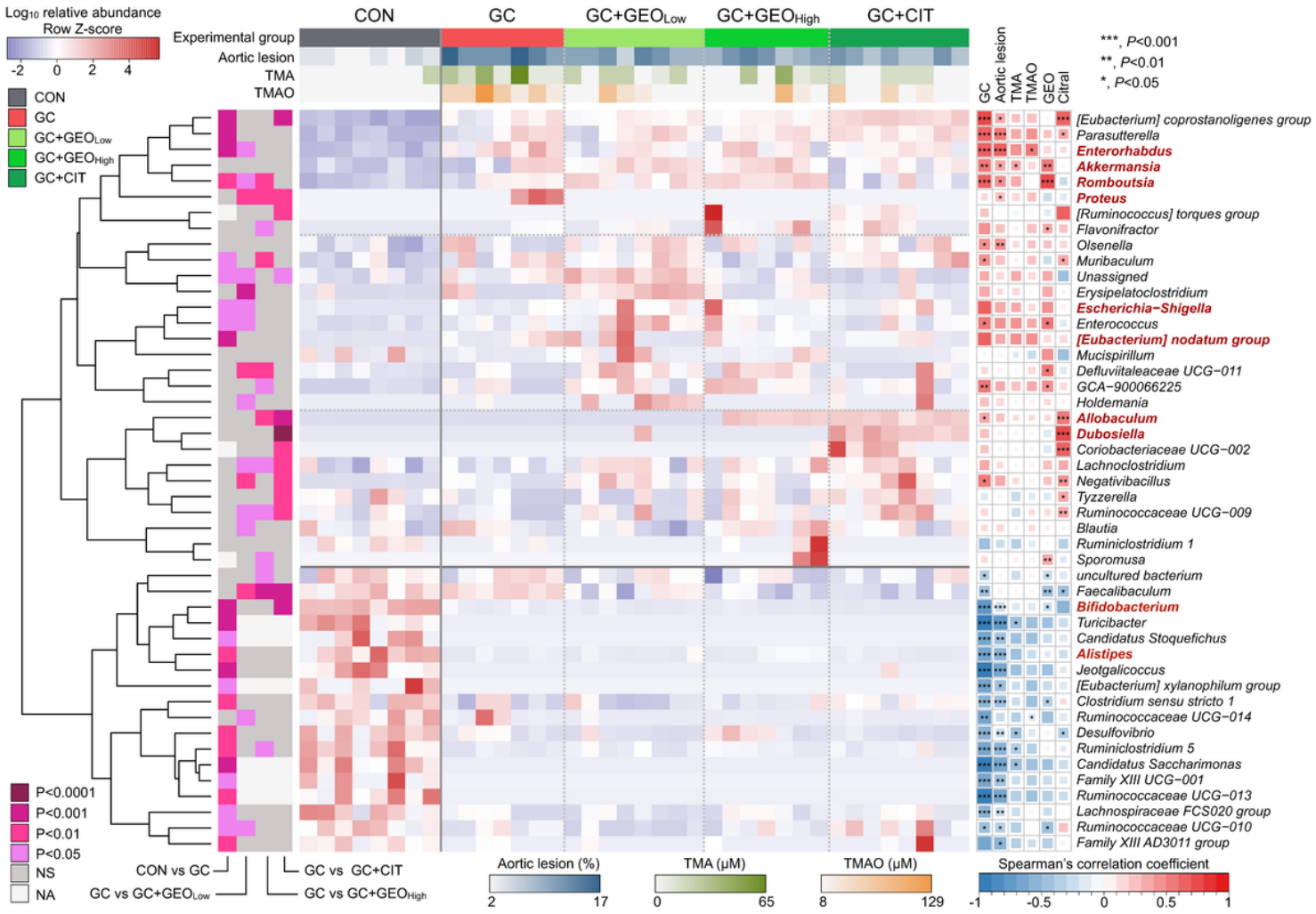

Figure 4

Remodelling of faecal microbiota at the genus level by GC, GEO, and citral, and their relationship with aortic lesion and gut microbiota metabolites. Heatmap for the relative abundance of significantly different faecal microbiota using the Kruskal–Wallis test (P< 0.05) and Spearman's correlation analysis between gut microbiota components at the genus level and aortic lesion and gut microbiota metabolites. Pairwise statistical analyses in the heatmap were performed using an unpaired Wilcoxon signed-rank test CON vs. GC groups; one-way ANOVA with Dunn's multiple comparison test for comparing GC, GC + GEO_{Low}, GC + GEO_{High}, and GC + CIT. GC: GAN with -carnitine diet, GEO: ginger essential oil

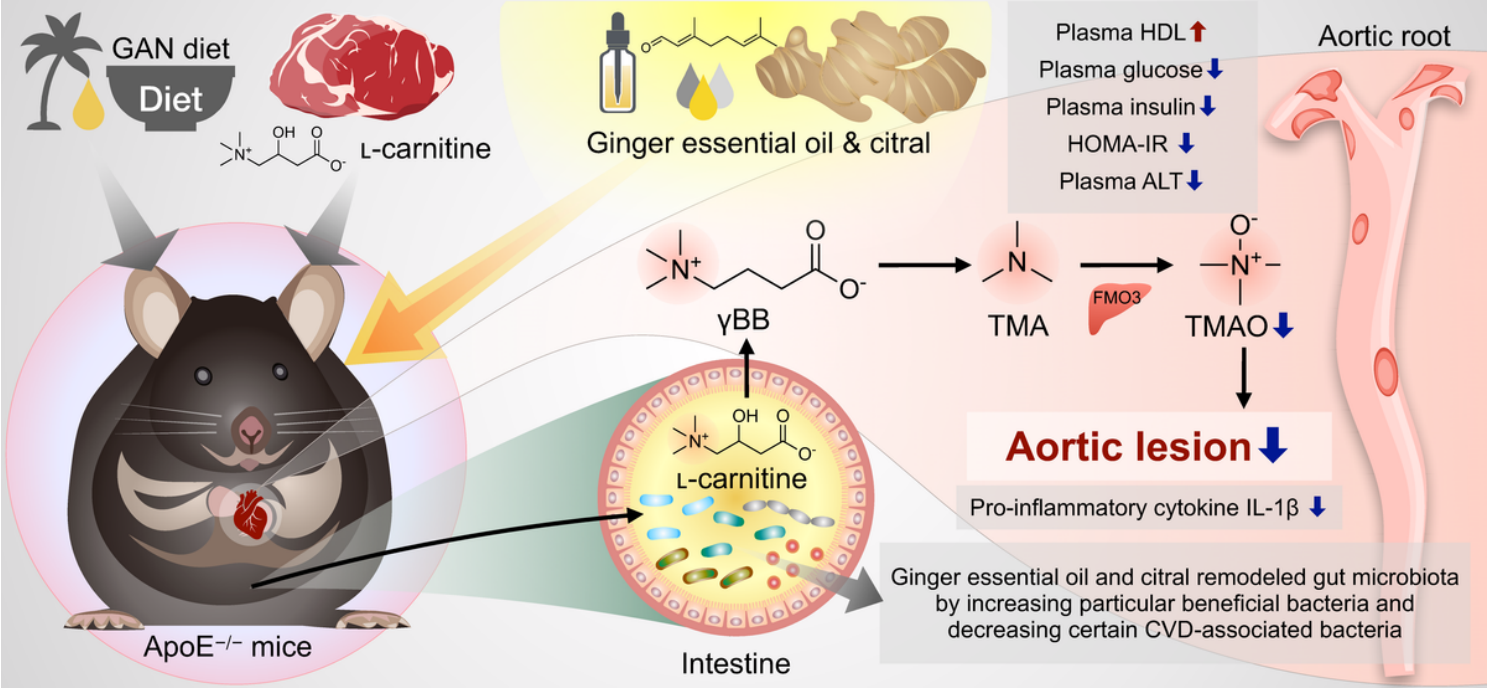

Figure 5

Effect of GEO and citral on cardiovascular disease prevention and atherosclerosis amelioration through gut microbiota and TMAO modulation. GEO and citral (1) protected ApoE-/- mice from GC-induced atherosclerosis and improved plasma lipidemic biomarker HDL; (2) enhanced glucose and insulin homeostasis, ameliorated the hepatic damage biomarker ALT, and lowered pro-inflammatory plasma cytokine IL-1β; (3) shaped the gut microbiota and down-regulated the metaorganismal metabolism of the -carnitine-TMAO pathway; and (4) favourably modulated the gut microbiota. GC: GAN with -carnitine diet, GEO: ginger essential oil, TMAO: trimethylamine-N-oxide

Supplementary Files

This is a list of supplementary files associated with this preprint. Click to download.

- SupplementaryFigureFinal.pdf